Bacteria Mediated Uranium Species Transformation and Immobilization Mechanism in a Phosphate-rich System

Wen-fa Tan

nhwftan@163.com

University of South China

Zhi-Wen Deng
University of South China

Jun-wen Lv
University of South China

Dong-shan Tang
University of South China

Jia-xiang Li
Chongqing University

Chao Pang
University of South China

Research Article

Additional Declarations: The authors declare no competing interests.

Abstract

Uranium tailings without reliable anti-seepage treatment in the early years of mining and metallurgy has become a potential source of pollution. This work sought to explore the transformation and mechanism of uranium species in a bacteria and phosphate coexist system. The results showed that addition of phosphate enhanced uranium removal rate greatly in solution with the highest removal rate of 99.84%. Likewise, BCR finding displayed that residual phase in sediment samples of phytic acid group and nano-hydroxyapatite group was much higher than that of control group. XRD/SEM-EDS analyses revealed that the fugitive positions of phosphorus and uranium elements remain essentially the same on the sediment surface in the groundwater-sediment system, the appearance of more pronounced phosphorus and uranium signal peaks confirmed more U-P precipitates. Combined with XPS and BCR results, very interesting, phosphate could be complexed with hexavalent uranium to form a stable precipitate. This, to some extent, do not seem to support the view that tetravalent uranium is only stable state under reducing conditions. From this point of view, it demonstrates that bacteria can effectively mediated U-P precipitates. This also provides theoretical evidence that it succeeds efficiently in realizing the transformation of uranium from a transferable phase to a stable phase, which has a potential application value to groundwater in uranium mining areas.

Introduction

Uranium pollutants downstream migration from uranium tailings are increasing without interruption (Knox et al. 2008, Xie et al. 2019). Presently, it has aroused a widespread concern of numerous countries on uranium contaminated water or soil (Cheng et al. 2022, Pereira et al. 2022).

Phosphate combines with uranium has been intensively investigated to form stable U-P precipitates or corresponding minerals (Chattanathan et al. 2013, Li et al. 2019, Simon et al. 2008). However, low permeability and migration of direct phosphate injection limit its practical application. Bacteria gradually decomposed organic phosphorus into phosphate via an enzymatic process, which may resolve the problem effectively in this mode (Tu et al. 2019). Indigenous bacteria, living in long-term uranium contamination, were able to reduce the metal stress by intensive phosphatase synthesis, benefiting a passive environmental remediation and playing a vital role in the biological chain (Boteva et al. 2016).

Considerable researches have described that *Pelosinus*, *Rahnella*, *Bacillus* or *Sphingomonas* could decompose sodium glycerophosphate into phosphate, which rapidly integrates with uranyl to form U-P biomineralization (Behera et al. 2017, Kong et al. 2020, Newsome et al. 2015, Shen et al. 2018). Indigenous *Bacillus, staphylococcus* and *Leifsonia* sp. isolated from uranium ore had a high accumulation capacity for UO_2^{+2} and could convert it into crystalline nano-uranium ore (Pan et al. 2015, Shukla et al. 2020, Tan et al. 2019). Previous efforts allowed the conclusion that bacteria facilitate the immobilization efficiency of uranium by changing the chemical states into less toxicity and less risky forms. It could, to some extent, prevent the migration and diffusion of uranium (Tan et al. 2020).

Whereas, the relevant study has only been done for a short period of time so far. Notably, Phosphate as a metal stabilizer in contaminated soils/sediments offers considerable potential for environmental cleanup.

Nevertheless, it's noting that phosphorus is also an essential element for the survival and growth of microorganisms. Sanchez-Castro pointed out that inorganic phosphates might also act as ligands in the presence of cations, such as uranyl ion, inducing the bioprecipitation of U(VI) as a protective strategy for bacteria (Sanchez-Castro et al. 2020). Since free orthophosphate is rarely found in certain environments, the main role of phosphatases is a primary converter supporting microbial nutrition by means of releasing assimilable orthophosphates from organic sources, which should be amended in case they are not naturally present. The question now is whether indigenous bacteria will be further decomposed and/or absorbed the U-P precipitates when system is short of phosphorus nutrients. Meanwhile, to a large degree, the mobility of uranium is subject to the redox reaction of the solid-liquid system (Belli &Taillefert 2018, Merroun &Selenska-Pobell 2008). Thus, as bacteria take up the phosphorus or especially when these bacteria decay and death, the stability of uranium has become a problem worthy of study.

This study mainly analyzed the morphological transformation and stability of uranium with aging time under the interaction of uranium, phosphorus and indigenous bacteria. Modified BCR extraction method was used to study the uranium speciation transformation. SEM-EDS, XRD and XPS were employed to analyze the product composition and uranium valence state.

Materials And Methods

Materials and reagents

Powdered U_3O_8 (AR, purchased from Hubei Chushengwei Chemical Co., Ltd) was used to prepare stock U(VI) solution ($1000mg \cdot L^{-1}$) (Wang et al. 2012). Uranium working solutions with concentrations of $10mg \cdot L^{-1}$ were obtained by diluting the stock solution. Phosphate reagents, phytic acid ($C_6H_{18}O_{24}P_6$) as an organic phosphorus source, nano-hydroxyapatite (nHAP) as an inorganic phosphorus source, were provided by Shanghai McLean Biochemical Technology Co., Ltd. *Staphylococcus* and *Bacillus* used in this work were initially isolated from an acidic uranium tailings near the town of Hengyang, China. Frozen bacterial liquid was thawed and added to the beef extract pep-tone culture medium with a pH of 7 ± 0.1 to activate and expand for 48 hours. Then they were divided into centrifuge tubes on the aseptic operating table. After centrifuge, the superannuate was poured out. The bottom sediments of the wet cells were served as experimental bacteria.

Experimental methods

Sample collection and preparation

Simulation groundwater-sediment system was prepared according to actual groundwater-sediment characteristics.

Composition of the simulated groundwater mainly referred to the research of Newsome and Wilkins (Newsome et al. 2014, Wilkins et al. 2007). Sediment sample was prepared with soil from an acidic uranium mining area near the town of Hengyang, China. The specific preparation process can consult our previous study (Tan et al. 2020). The concentrations of the designed substances are shown in Table 1. The pH of the

working solutions was adjusted initially with 1 mol·L^{-1} hydrochloric acid or 1 mol·L^{-1} sodium hydroxide (aq). N_2 was used to ensure the groundwater-sediment system of anoxic atmosphere. Experiment was conducted in a glove box at room temperature under nitrogen protection.

Table 1
Content of simulated groundwater-sediment

Component	Sediments mg·kg^{-1}	Ground water mg·L^{-1}
Fe^{3+}	-	50.00
Ca^{2+}	-	150.00
Mg^{2+}	-	50.00
K^+	-	100.00
Na^+	-	50.00
U	140.00	10.00(VI)
Cl^-	-	250.00
NO^{3-}	-	50.00
$CO_3{}^{2-}$	-	50.00
$SO_4{}^{2-}$	-	1040.00
pH	-	6.00

Uranium immobilization experiments

A series of experiments were carried out to investigate the effect of bacteria mediated phosphate on uranium immobilization.

The experiment was divided into three groups: (1) control group (CK) which only added bacteria (0.30g·L^{-1}); (2) phytic acid ($C_6H_{18}O_{24}P_6$) as experimental group added bacteria and phytic acid; (3) nano-hydroxyapatite (nHAP) as another experimental group added bacteria and nano-hydroxyapatite. The jars were disinfected and sterilized before adding the bacteria. Three parallel samples were set in each group.

Analysis and testing methods

Solid-phase morphologies of uranium in sediment samples were analyzed by an improved BCR sequential extraction (Baker et al. 2019, Ding et al. 2018).

Sediment samples was prepared for analysis at 48th and 1080th hour. The obtained deposits were baked in a vacuum drying oven at a temperature of 60°C for 12 hours. Accurately 0.50g of dry sediment samples

were weighed to conduct BCR sequential extraction analysis. Extraction step is showed in Table 2 (Nemati et al. 2011).

Table 2
Sequential extraction procedure for element partitioning assessment

Extraction step	Target phase (s)	Reagent (s)	Experimental methods
1	Soil solution, carbonates, exchangeable metals	HOAc 20.00mL 0.11mol·L^{-1}	Oscillating in a water bath at 30°C for 16 hours, centrifuging (7000r·min^{-1},10min)
2	Oxides Fe/Mn	$NH_2OH·HCl$ 20.00mL 0.50mol·L^{-1}	Oscillating in a water bath at 30°C for 16 hours, centrifuging (7000r·min^{-1},10min)
3	Organic matter and sulphides	30.00% H_2O_2 5.00 + 5.00mL	Digesting for 1 hour at room temperature + Heating in water bath at (82 ± 2) °C environment for 1 hour
		NH_4OAc 25.00mL 1.00mol·L^{-1}	Oscillating in a water bath at 30°C for 16 hours, centrifuging (7000r·min^{-1},10min)
4	Soil solution, carbonates, exchangeable metals	$HCl + HNO_3 +$ hydrochloric acidO_4	Digestion

Uranium concentration, phosphorus concentration and ferrous ion concentration were measured by UV spectrophotometer. All experiments were repeated three times. The precipitation products were analyzed by SEM-EDS, XRD and XPS techniques at 360th hour.

Results And Discussion

Variations of groundwater-sediment parameters

Figure 1 brings out parameter changes of uranium, pH, ORP, and phosphate and Fe concentration during the experiment.

It can be seen from Fig. 1a that the uranium removal rate of control group reached 90% in 4th hours then followed by desorption release. This indicates that uranium adsorption by bacteria is unstable. The trend of the experimental group was opposite which argues phosphate plays an irreplaceable and vital role in this process. Percentage of uranium removed of nHAP group rocketed rapidly from 19.71−86.46% in 120th hours, even the uranium concentration in the solution was below the limit of detection at 480th hour. Perhaps, the increased release of phosphate ions from nHAP dissolution is on account of pH and ORP value

of the system. It is interesting to note that at this stage, the dominance of complexation may explain the elevated remove rate of uranium (Liu et al. 2020). In the $C_6H_{18}O_{24}P_6$ group, the removal rate of uranium is steadily rising and finally stabilize at 99%. Combined with the variation of phosphate concentration in Fig. 1d, a conclusion could be safely drawn that *Staphylococcus* and *Bacillus* are able to decompose gradually $C_6H_{18}O_{24}P_6$ into orthophosphate which in turn facilitates the removal of uranium.

Chemical states of uranium in the precipitates

The improved BCR sequential extraction method was used to analyze the uranium species in view of this characteristic. According to the previous studies, exchangeable uranium, mainly composed of water-soluble and exchangeable substances, such as free acyl ions and weakly adsorbed uranium, was more vulnerable to external factors and released into the environment, which has more potential threats to surroundings (Echevarria et al. 2001, Vandenhove et al. 2014). On the contrary, residual uranium, under natural conditions, was arduous to release and could exist in sediments for long periods of time without causing environmental damage. Figure 2 visually presents that the chemical states of uranium changed in different degrees after anoxic culture for 480th hour and 1080th hour.

Table 3 expresses the specific data changes of uranium speciation. It can be seen that uranium in an unstable state especially exchangeable fraction in control group accounts for a large proportion. The exchangeable state of control group increased by $8.73 mg \cdot kg^{-1}$ from 480th hour to 1080th hour. The content of exchangeable phase in phytic acid group and nano-hydroxyapatite group is much lower than that in control group. Also, the residual state in phytic acid group with a difference of nearly $60.00 mg \cdot kg^{-1}$ in comparison with the control group.

Table 3
Proportions of various uranium species in samples at 480th and 1080th hour (%)

Time	Target phase(s)	CK		$C_6H_{18}O_{24}P_6$		nHAP	
		mg•kg^{-1}	Total weight %	mg•kg^{-1}	Total weight %	mg•kg^{-1}	Total weight %
480h	Acid extractable/exchangeable fraction	36.63	26.16	-2.86	-2.04	7.01	5.01
	Easily reducible fraction	27.52	19.65	-1.91	-1.37	6.06	4.33
	Oxidizable fraction	13.40	9.57	18.85	13.46	12.26	8.76
	Residual fraction	62.45	44.61	125.93	89.95	114.66	81.90
1080h	Acid extractable/exchangeable fraction	45.36	32.40	2.26	1.62	10.75	7.68
	Easily reducible fraction	27.39	19.56	5.18	3.70	11.63	8.31
	Oxidizable fraction	13.91	9.94	21.50	15.36	6.95	4.96
	Residual fraction	53.34	38.10	111.06	79.33	110.68	79.05

Analysis of uranium speciation

SEM and EDS analysis

Figure 3 shows the microscopic morphology, structure and surface elements of sediment samples characterized by scanning electron microscopy and energy dispersive spectroscopy, respectively. As shown in Fig. 3a, the amount of particle size in CK group is small, and loose. Different from the control group, the product structure of experimental group was an irregular large block-like precipitate (Fig. 3c, e), and the surface is much rougher than that of Ck group. The EDS spectra element content analysis indicated that the block-like precipitates maybe U-P minerals as a clear peak of phosphorus and uranium displayed in Fig. 3d and Fig. 3f.

XRD patter analysis

It can be discovered from Fig. 4 that SiO_2 is the main phase composition in the samples (Li et al. 2021). The position of diffraction peak is roughly similar in different experimental groups. A weak $Ca_5(PO_4)_3OH$ (PDF#08-0313) peak and $(UO_2)_4O(OH)_6(H_{20})_5$ (PDF#70-4765) peak appear separately (Fig. 4). U-P peaks not be detected probably in that the U-P precipitate is not crystallization or in amorphous crystals form or weak crystalline form, both of which happens to highly difficult to be detected via XRD (Zhang et al. 2020).

XPS analysis

In order to determine the chemical valence state of uranium, XPS analysis was performed at 360th hour. The results are shown in Fig. 5. The peak of U4f$_{7/2}$ (377.40-378.30eV) and U4f$_{5/2}$ (391.40-392.60eV) are both about 14.00-10.60 eV energy separation (Xie et al. 2020). The separation was decomposed into two groups of peaks, indicating that U existed in two chemical states.

The specific parameters are shown in Table 4. It displays that the proportion of U(IV) and U(VI) in C$_6$H$_{18}$O$_{24}$P$_6$ group and nHAP group is 75.70%, 25.30%, and 89.57%, 10.43%, respectively. Tetravalent uranium is commonly assumed to form insoluble species, resulting in the immobilization of uranium under reducing conditions. From this point of view, it indicates that the immobilization effect of insoluble phosphate is more idealized compared with the former. However, combined with BCR result, the experimental data of uranium chemical states do not seem to support this point. This, in some ways, agrees with this viewpoint that phosphate can be complexed with hexavalent uranium to form a stable precipitate.

Table 4
Statistical table of XPS peak parameters of uranium

Sample	Fitting Parameters	U4f$_{7/2}$			U4f$_{5/2}$			Atom/at%
		B.E./eV	FWHM	Area	B.E./eV	FWHM	Area	
C$_6$H$_{18}$O$_{24}$P$_6$	U( )	378.30	2.85	2409.51	391.40	1.26	605.46	75.70%
	U( )	381.90	3.27	867.20	392.60	0.50	153.76	25.30%
nHAP	U( )	377.40	3.78	5378.23	391.40	1.26	327.35	89.57%
	U( )	382.00	2.82	614.52	392.60	0.50	49.84	10.43%

Conclusions

The bacterially mediated U(VI) biomineralization has a better stabilizing effect in anoxic atmosphere, and will be a supplementary technology for the treatment of uranium-contaminated groundwater-sediment. This work ascertained that the addition of phosphate not only provides electron donors, but also greatly promoted the stable of uranium. The products of uranium precipitate may be U-P precipitates and calcium-bearing minerals. In addition, the findings explain that bacteria may facilitate phosphate complexed with hexavalent uranium to form a stable precipitate. In some sense, it seems to support the argue that tetravalent uranium is merely a stable phase under reductive condition. From this perspective, it implies that bacteria can effectively mediated U-P precipitates. Further efforts will be devoted to determining the mechanism of uranium uptake and transport by bacteria, so that to obtain a comprehensive explanation for the formation of uranium biominerals.

Declarations

Ethical Approval

The authors declare that they have no conflict of interest.This article does not contain any studies with human participants or animals performed by any of the authors.

Consent to Participate

Not applicable

Consent to Publish

Not applicable

Author Contributions

All authors contributed to the study conception and design. Material preparation, data collection and analysis were performed by Jinzhi Cun, Wenfa Tan Peng Lei and Chao Pang. The first draft of the manuscript was written by Jinzhi Cun and all authors commented on previous versions of the manuscript. All authors read and approved the final manuscript.

Competing Interests

The authors have no financial or proprietary interests in any material discussed in this article.

Availability of data and materials

Not applicable

References

1. Baker MR, Coutelot FM, Seaman JC (2019) Phosphate amendments for chemical immobilization of uranium in contaminated soil. Environ Int 129:565–572
2. Behera BC, Yadav H, Singh SK, Mishra RR, Sethi BK, Dutta SK, Thatoi HN (2017) Phosphate solubilization and acid phosphatase activity of Serratia sp. isolated from mangrove soil of Mahanadi river delta, Odisha, India. J Genet Eng Biotechnol 15:169–178
3. Belli KM, Taillefert M (2018) Geochemical controls of the microbially mediated redox cycling of uranium and iron. Geochim Cosmochim Acta 235:431–449
4. Boteva S, Radeva G, Traykov I, Kenarova A (2016) Effects of long-term radionuclide and heavy metal contamination on the activity of microbial communities, inhabiting uranium mining impacted soils. Environ Sci Pollut Res Int 23:5644–5653

5. Chattanathan SA, Clement TP, Kanel SR, Barnett MO, Chatakondi N (2013) : Remediation of Uranium-contaminated Groundwater by Sorption onto Hydroxyapatite Derived from Catfish Bones. Water, Air, & Soil Pollution 224

6. Cheng C, Chen L, Guo K, Xie J, Shu Y, He S, Xiao F (2022) Progress of uranium-contaminated soil bioremediation technology. J Environ Radioact 241:106773

7. Ding L, Tan WF, Xie SB, Mumford K, Lv JW, Wang HQ, Fang Q, Zhang XW, Wu XY, Li M (2018) Uranium adsorption and subsequent re-oxidation under aerobic conditions by Leifsonia sp. - Coated biochar as green trapping agent. Environ Pollut 242:778–787

8. Echevarria G, Sheppard MI, Morel J (2001) Effect of pH on the sorption of uranium in soils. J Environ Radioact 53:257–264

9. Knox AS, Brigmon RL, Kaplan DI, Paller MH (2008) Interactions among phosphate amendments, microbes and uranium mobility in contaminated sediments. Sci Total Environ 395:63–71

10. Kong L, Ruan Y, Zheng Q, Su M, Diao Z, Chen D, Hou L, Chang X, Shih K (2020) Uranium extraction using hydroxyapatite recovered from phosphorus containing wastewater. J Hazard Mater 382:120784

11. Li J, Pang Z, Zhou S, Li Z, Rong L, Xiao J, Liu Y, Tian L, Chu L (2021) Immobilization of uranium soil with nHAP and composite. Res Chem Intermed 47:2985–3004

12. Li R, Ibeanusi V, Hoyle-Gardner J, Crandall C, Jagoe C, Seaman J, Anandhi A, Chen G (2019) Bacterial-facilitated uranium transport in the presence of phytate at Savannah River Site. Chemosphere 223:351–357

13. Liu G, Liao B, Lu T, Wang H, Xu L, Li Z, Ye C (2020) : Insight into immobilization of Pb^{2+} in aqueous solution and contaminated soil using hydroxyapatite/attapulgite composite.Colloids and Surfaces A: Physicochemical and Engineering Aspects603

14. Merroun ML, Selenska-Pobell S (2008) Bacterial interactions with uranium: an environmental perspective. J Contam Hydrol 102:285–295

15. Nemati K, Abu Bakar NK, Abas MR, Sobhanzadeh E (2011) Speciation of heavy metals by modified BCR sequential extraction procedure in different depths of sediments from Sungai Buloh, Selangor, Malaysia. J Hazard Mater 192:402–410

16. Newsome L, Morris K, Lloyd JR (2014) The biogeochemistry and bioremediation of uranium and other priority radionuclides. Chem Geol 363:164–184

17. Newsome L, Morris K, Trivedi D, Bewsher A, Lloyd JR (2015) Biostimulation by Glycerol Phosphate to Precipitate Recalcitrant Uranium(IV) Phosphate. Environ Sci Technol 49:11070–11078

18. Pan X, Chen Z, Chen F, Cheng Y, Lin Z, Guan X (2015) The mechanism of uranium transformation from U(VI) into nano-uramphite by two indigenous Bacillus thuringiensis strains. J Hazard Mater 297:313–319

19. Pereira WS, Kelecom A, Charles-Pierre M, Lopes JM, Campelo ELC, Espindola CB, Carmo AS, Junior DAP, Pelegrineli SQ, Silva AX (2022) Assessment of released natural radionuclides by waste rock pile and mining pit associated with a uranium mine at Caldas, Minas Gerais, Brazil. Environ Sci Pollut Res Int 29:58065–58077

20. Sanchez-Castro I, Martinez-Rodriguez P, Jroundi F, Solari PL, Descostes M, Merroun ML (2020) High-efficient microbial immobilization of solved U(VI) by the Stenotrophomonas strain Br8. Water Res 183:116110

21. Shen Y, Zheng X, Wang X, Wang T (2018) The biomineralization process of uranium(VI) by Saccharomyces cerevisiae - transformation from amorphous U(VI) to crystalline chernikovite. Appl Microbiol Biotechnol 102:4217–4229

22. Shukla SK, Hariharan S, Rao TS (2020) Uranium bioremediation by acid phosphatase activity of Staphylococcus aureus biofilms: Can a foe turn a friend? J Hazard Mater 384:121316

23. Simon FG, Biermann V, Peplinski B (2008) Uranium removal from groundwater using hydroxyapatite. Appl Geochem 23:2137–2145

24. Tan W, Guo F, Deng Q, Li J, Wang L (2019) The effects of Leifsonia sp. on bioavailability and immobilization mechanism of uranium in soil. J Soils Sed 20:1599–1608

25. Tan WF, Li Y, Guo F, Wang YC, Ding L, Mumford K, Lv JW, Deng QW, Fang Q, Zhang XW (2020) Effect of Leifsonia sp. on retardation of uranium in natural soil and its potential mechanisms. J Environ Radioact 217:106202

26. Tu H, Yuan G, Zhao C, Liu J, Li F, Yang J, Liao J, Yang Y, Liu N (2019) U-phosphate biomineralization induced by Bacillus sp. dw-2 in the presence of organic acids. Nucl Eng Technol 51:1322–1332

27. Vandenhove H, Vanhoudt N, Duquene L, Antunes K, Wannijn J (2014) Comparison of two sequential extraction procedures for uranium fractionation in contaminated soils. J Environ Radioact 137:1–9

28. Wang Y-Q, Zhang Z-B, Liu Y-H, Cao X-H, Liu Y-T, Li Q (2012) Adsorption of U(VI) from aqueous solution by the carboxyl-mesoporous carbon. Chem Eng J 198–199:246–253

29. Wilkins MJ, Livens FR, Vaughan DJ, Beadle I, Lloyd JR (2007) The influence of microbial redox cycling on radionuclide mobility in the subsurface at a low-level radioactive waste storage site. Geobiology 5:293–301

30. Xie Y, Chen C, Ren X, Wang X, Wang H, Wang X (2019) Emerging natural and tailored materials for uranium-contaminated water treatment and environmental remediation. Prog Mater Sci 103:180–234

31. Xie Y, Fang Q, Li M, Wang S, Luo Y, Wu X, Lv J, Tan W, Wang H, Tan K (2020) Low concentration of Fe(II) to enhance the precipitation of U(VI) under neutral oxygen-rich conditions. Sci Total Environ 711:134827

32. Zhang W, Liu H, Fan X, Zhuo Z, Guo Y (2020) : Removal of uranium from aqueous solution by a permeable reactive barrier loaded with hydroxyapatite-coated quartz sand: Implication for groundwater remediation. Geochemistry 80
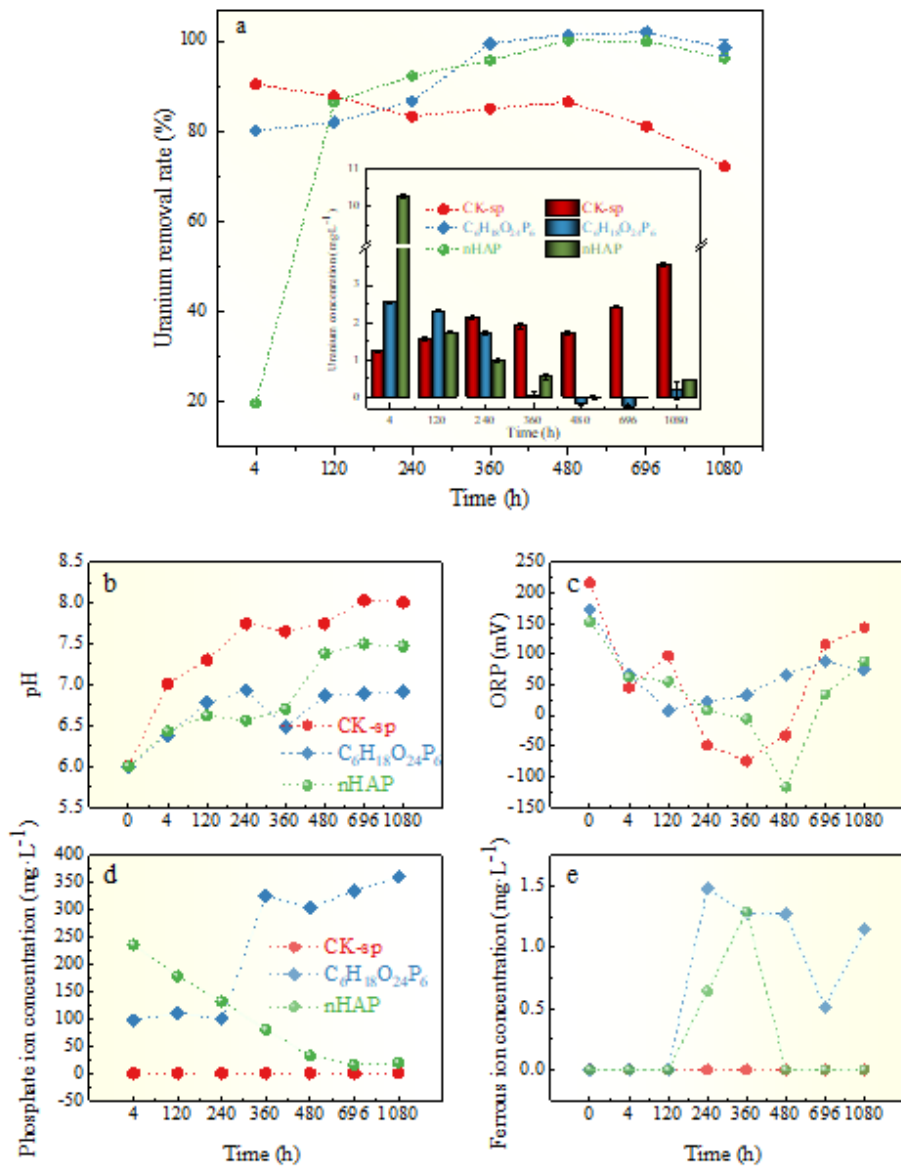
Figures

Figure 1

Variations of (a) uranium concentration, (b) pH, (c) ORP, (d) phosphate and (e) ferrous ion concentrations in reaction system
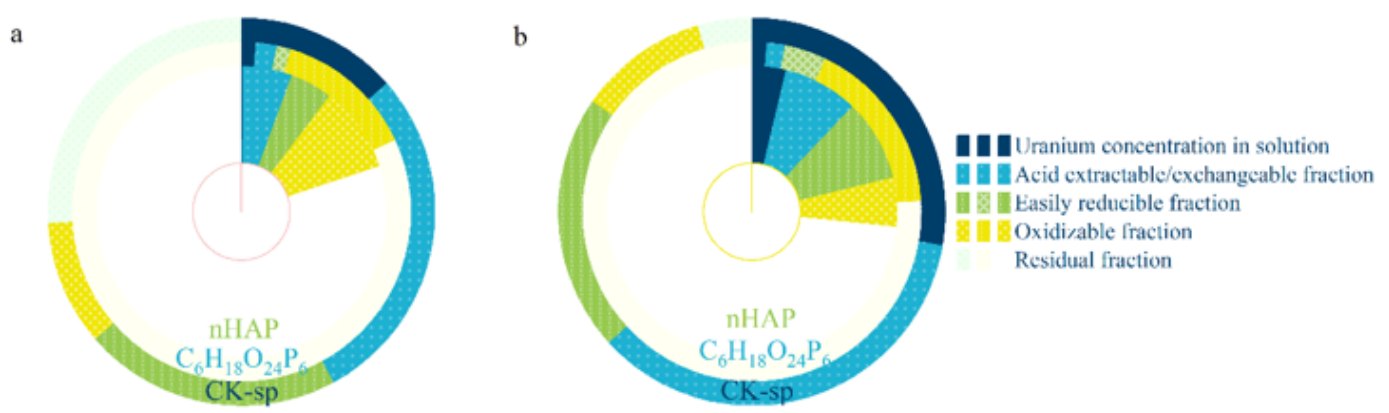
Figure 2

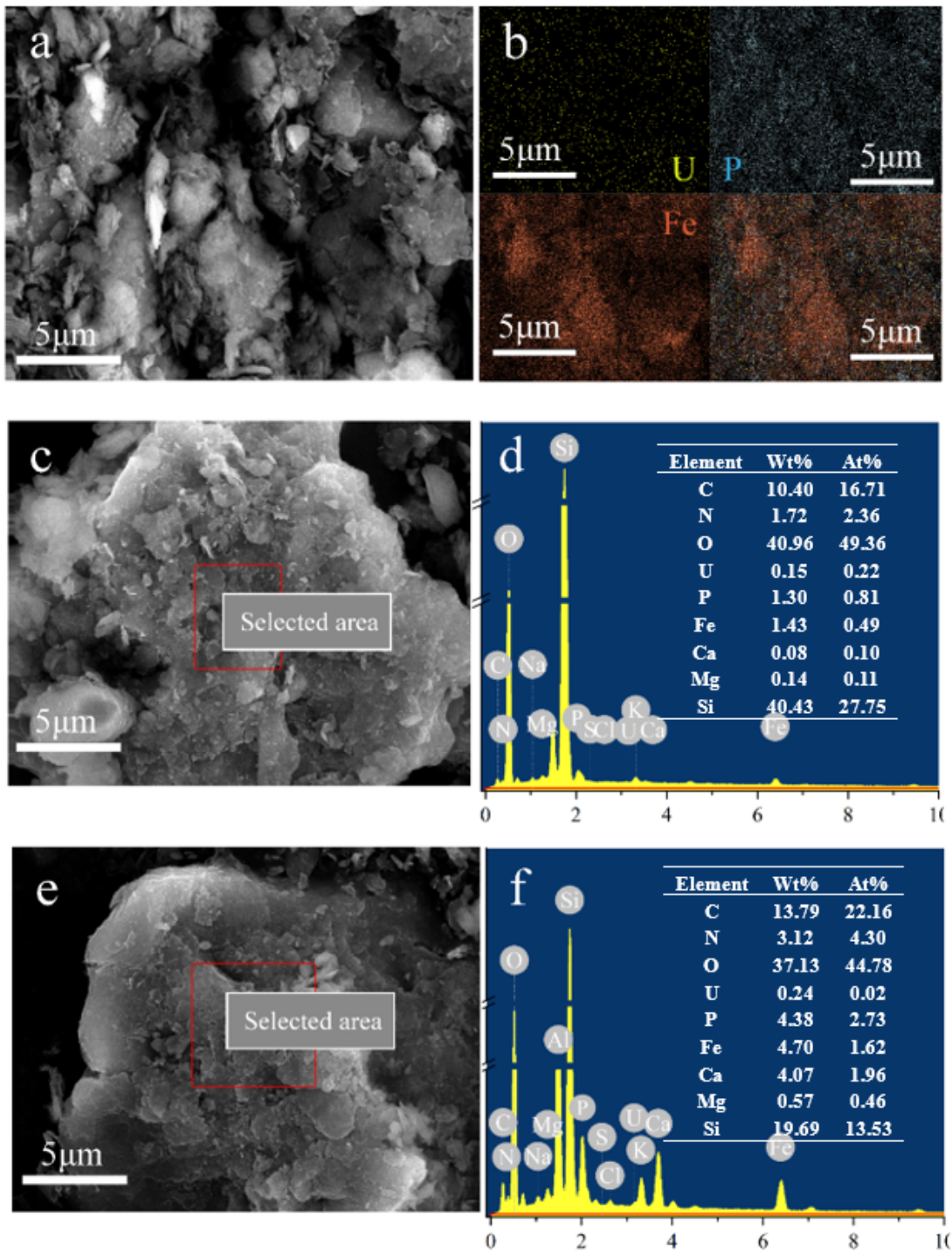The chemical states of uranium incubated at (a) 480th hour, and (b) 1080th hour

Figure 3

SEM and EDS images of sediment samples at 360th hour incubation, (a, b) CK group, (c, d) $C_6H_{18}O_{24}P_6$ group, (e, f) nHAP group
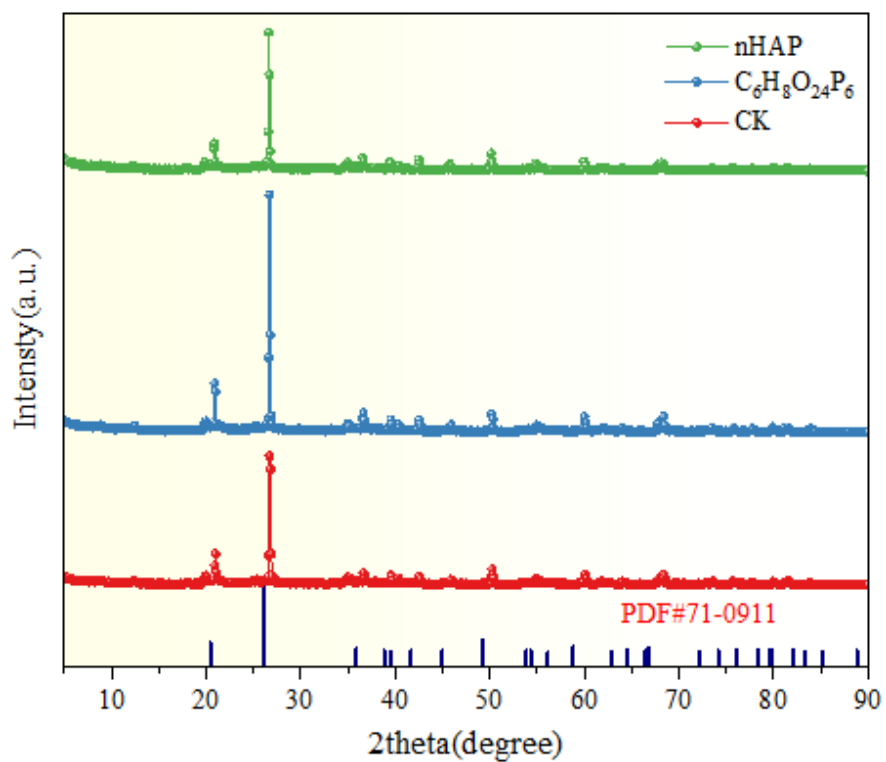
Figure 4

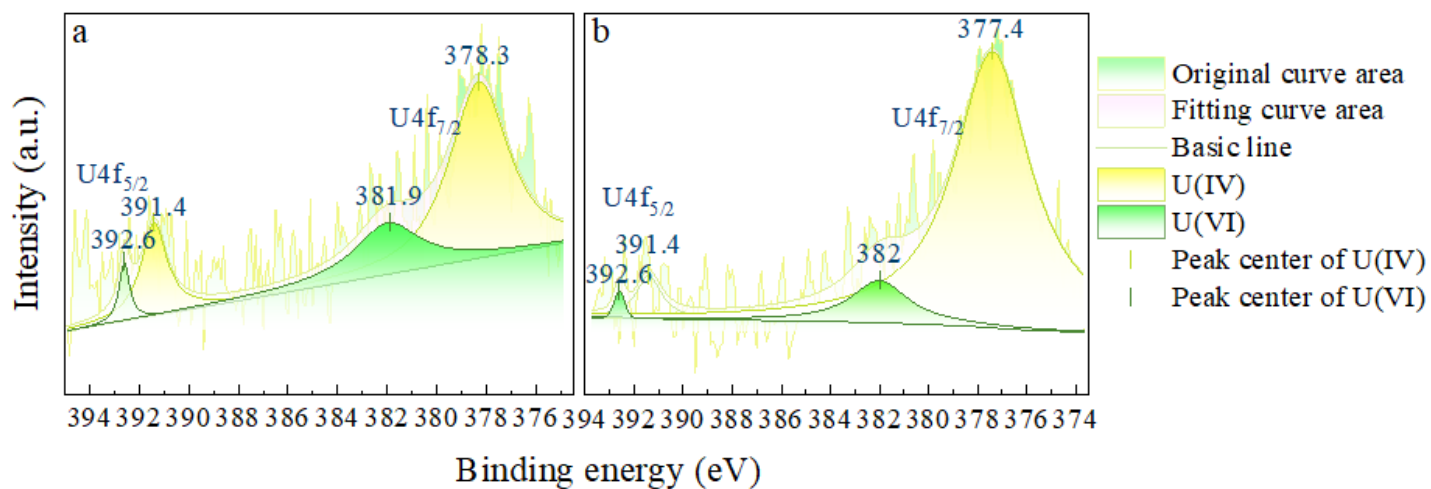XRD spectra of sediment samples

Figure 5

XPS spectra of uranium at 360th hour, (a) $C_6H_{18}O_{24}P_6$ group, (b) nHAP group